Observation of shells in Coulomb explosions of rare-gas clusters

B. Erk, K. Hoffmann, N. Kandadai, A. Helal, J. Keto, and T. Ditmire*

Texas Center for High Intensity Laser Science, Department of Physics, The University of Texas at Austin, Austin, Texas 78712, USA

(Received 27 August 2010; published 11 April 2011)

The explosions of noble gas clusters from argon and xenon irradiated by intense 35-fs infrared laser pulses have been studied. The kinetic energy spectra of ions produced in small clusters (<700 atoms) show a two-mode shell structure that is attributed to originating from a radial charge distribution. With a simple classical particle simulation of Coulomb explosions, the energy structure was reproduced using information on the arrangement of charge in the cluster. It was found that, during the explosion, the inner atoms of the clusters were less ionized than the outer atoms.

DOI: 10.1103/PhysRevA.83.043201 PACS number(s): 36.40.Qv, 36.40.Vz, 36.40.Mr, 36.40.Gk

I. INTRODUCTION

Rare-gas clusters are ideal model systems to study the size-dependent properties of matter as they have a high local absorption while maintaining an overall high transmission. Irradiated by intense laser pulses, they generate energetic particles and radiation. The dynamics of these processes is well studied but yet not completely understood.

There are two general models that describe the interaction of intense infrared laser pulses with a cluster of atoms. For small clusters, the free electrons escape from the ions in the cluster and leave bare, highly charged ions behind that repel each other by Coulomb forces and thus explode very rapidly [1]. This Coulomb explosion behavior was also confirmed for diatomics and small polyatomic molecules [2,3].

Ditmire *et al*. [4,5] showed that this picture is not valid for big clusters. They introduced a hydrodynamic model and suggested that the explosion of the ions in the cluster is very much like that observed in the hot electron-driven expansion of a laser-heated solid target plasma. In the model, some of the electrons are confined by space-charge forces forming a nanoplasma in the center of the cluster that expands more slowly by the pressure of the energetic electrons. A detailed hydrodynamic model was published later by Milchberg *et al*. [6].

II. EXPERIMENT

The ultrashort infrared laser pulses for the experiment were produced by the Texas High-Intensity Optical Research Laser (THOR) system. This is a Ti:sapphire CPA system producing 35-fs pulses with a wavelength centered near 800 nm operating at a repetition rate of up to 10 Hz. A small fraction of the maximum energy was focused by a $f/10$ spherical mirror in a close-to-normal incidence configuration. The laser intensity was calibrated from beam parameters and atomic ionization yields measured by Larochelle *et al*. [7]. For all experiments, the focal intensity was kept constant at 5×10^{15} W/cm^2. A modified pulsed, gas-jet nozzle (General Valve, Series 9), with a 15° half cone opening and a throat diameter of 500 μm, was used to produce a jet of noble gas clusters perpendicular to the laser propagation. The cluster beam was collimated using a differential pumping scheme with a conical beam skimmer, which had an orifice diameter of 1.5 mm. The average size $\langle N \rangle$ of the produced clusters was estimated from scattering measurements [8] and according to parameters given by Hagena *et al*. [9] and Dorchies *et al*. [10]. Their size distribution was assumed log-normal [11].

To measure the ionized cluster fragments, a Wiley-McLaren time-of-flight (TOF) mass spectrometer [12], as shown in Fig. 1, was used. The overall TOF length was 370 mm, and a 5-mm opening in the extraction plate allowed extraction from the focal volume. The ions were detected using microchannel plates (MCP) in a chevron configuration and recorded with a digital oscilloscope. The spectrometer was used in two configurations. The first setup had charged extraction grids around the laser-cluster interaction area, followed by an extended acceleration region and the field-free drift region toward the detector. The second setup was with the extraction grids at ground, which provided a single field-free drift region allowing the ions from the cluster expansion to travel to the MCP detector. Knowing the mass of the ions and their flight times, the kinetic energy could be reconstructed, providing a way to investigate the energy spectra from the cluster expansions.

III. EXPERIMENTAL DATA

Time-of-flight mass spectra of laser-cluster interaction products are presented in Fig. 2. The laser intensity was held constant at of 5×10^{15} W/cm^2, while the cluster size was varied. The spectra show high-charge states and kinetic energy both for argon and xenon cluster explosions. The energy of the produced ions increases with the size of the clusters.

For the lower-charge ions, this can be observed from the peak broadening of the characteristic three-folded peak structure. Dashed lines are used to guide the evolving kinetic energy. This structure results from the design of the extraction mechanism described before. The earlier peak in time results from the ions that reach the detector directly (forward-exploding ions), whereas the later peak represents the ions that at first fly away from the detector, but then stopped and reversed toward the detector by the extraction field [backward-reflected ions (see Fig. 1)]. According to Wiley and McLaren [12], the time difference Δt between those two peaks is proportional to the initial kinetic energy of the ions $E_{\text{ion}} \sim (q \Delta U \Delta t)^2$, which is highly dependent on the extraction voltage ΔU between the

*Corresponding author: tditmire@physics.utexas.edu

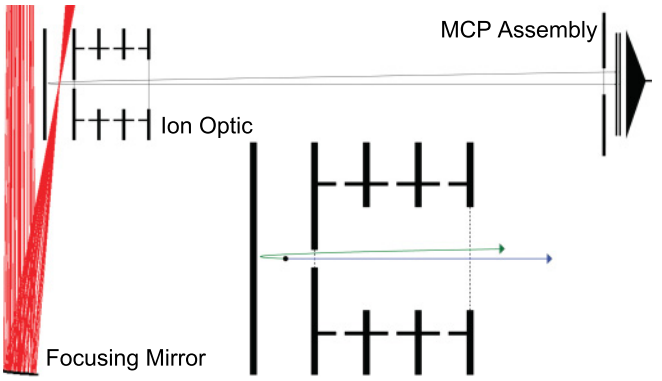

FIG. 1. (Color online) Illustration of the laser-cluster experiment. Ions from cluster explosions are extracted from the laser focus into a TOF assembly. Only ions traveling parallel and antiparallel to the TOF axis are detected as shown; all other ions are rejected by the aperture in the ion optic.

extraction grids. The center peak is generated by low-energy ions, e.g., those from background atoms, small clustered beam constituents, or are produced in charge exchange [13].

For higher-charged ions, the peak broadening led to overlapping structures toward shorter ion arrival times. The broad peak structure observed for larger clusters sizes between 3 and 5 μs in Fig. 2(a) also originates from higher-charge states with kinetic energy higher than the extraction voltage. This smears the flight times, and the peaks can not be resolved and identified. That makes the extraction of kinetic energy from peak splittings incomplete and limited by the extraction voltage used. To get information about the kinetic energies of the ions produced in the cluster expansion process beyond the energies that can be determined with the above-described peak-splitting method, the second, more direct energy measurement described above for different cluster sizes was used. With that, however, charge information in the spectra is lost.

Figure 3 shows kinetic ion energy distributions derived from TOF spectra with no extraction fields for argon and xenon clusters of different average sizes taken at the same laser intensity of 5×10^{15} W/cm^2. In this field-free setup, the ion collection efficiency is reduced and we were not able to measure a signal in a reasonable time for cluster sizes below 200 atoms. For large clusters, high-energy ions above 20 keV are observed. Because of its higher condensation rate, xenon forms bigger clusters and, for the same cluster size, it also produces ions with larger kinetic energies compared to argon. It is also observed that xenon has a greater number of low-energy ions. This results in a difference in the kinetic energy TOF peak shape between argon and xenon. More significant is the observation of a double peak structure in energy for both gases for small clusters (<700 atoms). A similar structure was observed in model calculations for high-intensity laser interaction with a 55-atom Ar cluster and was attributed to nonuniform ionization, which led to the formation of ion shells during the cluster explosion [14].

IV. MODEL

To verify this idea, simple classical particle simulations of Coulomb explosions were performed to obtain an energy

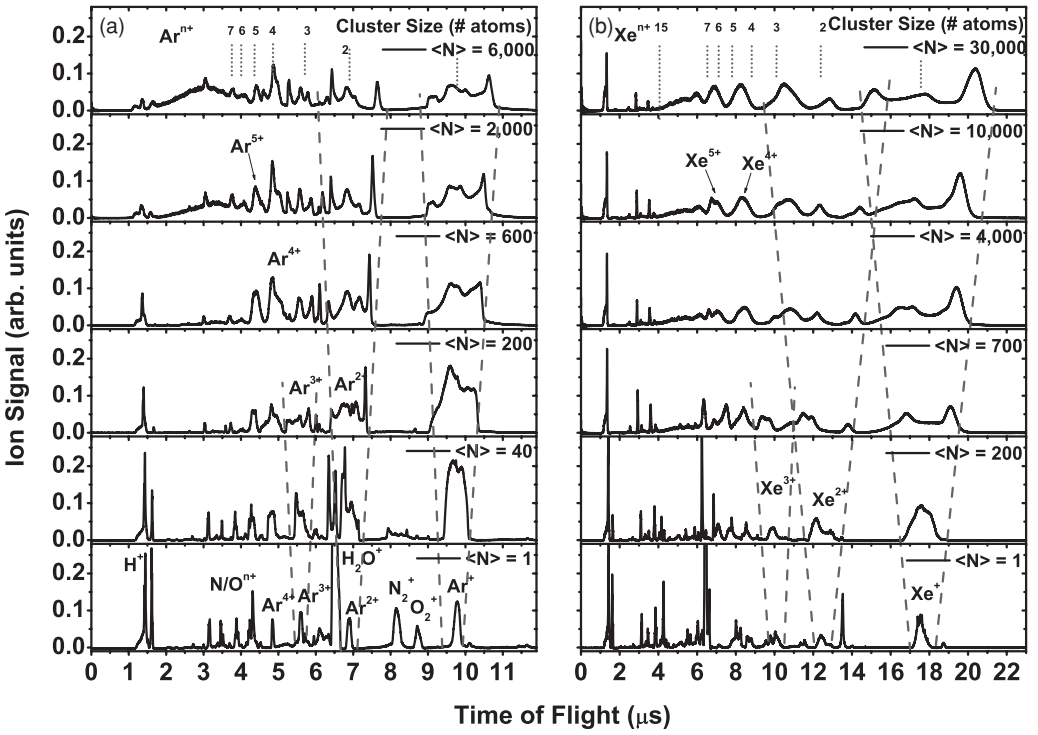

FIG. 2. Time-of-flight spectra of ions originating from various (a) Ar and (b) Xe cluster sizes at a constant laser intensity of 5×10^{15} W/cm^2. The atomic spectra are background dominated by O_2, N_2, and H_2O ions; they vanish as the gas-jet pressure is increased. Cluster spectra show high-charge states and kinetic energy from cluster explosions. Vertical dotted lines show expected arrival times for multiple charged ions. Dashed lines guide the peak broadening for lower-charged ions caused by kinetic energy.

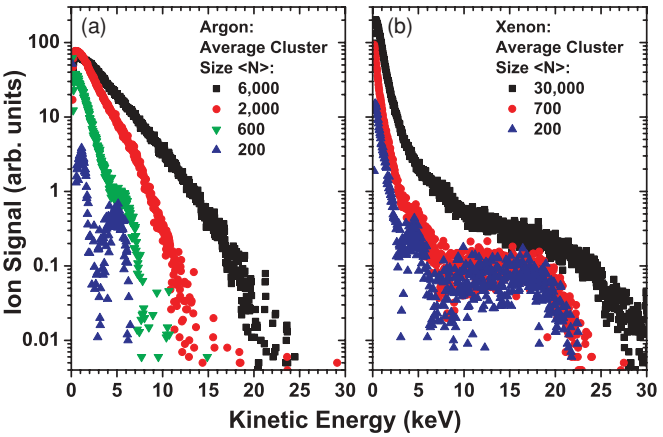

FIG. 3. (Color online) Ion kinetic energy spectra derived from a field-free TOF setup. (a) Ar and (b) Xe cluster sizes were varied at a constant laser intensity of 5×10^{15} W/cm^2. The kinetic energy of the ions increases with cluster size. Small clusters show a double peak structure in the energy distribution, which results from an inhomogeneous charge distribution and shell-wise explosion.

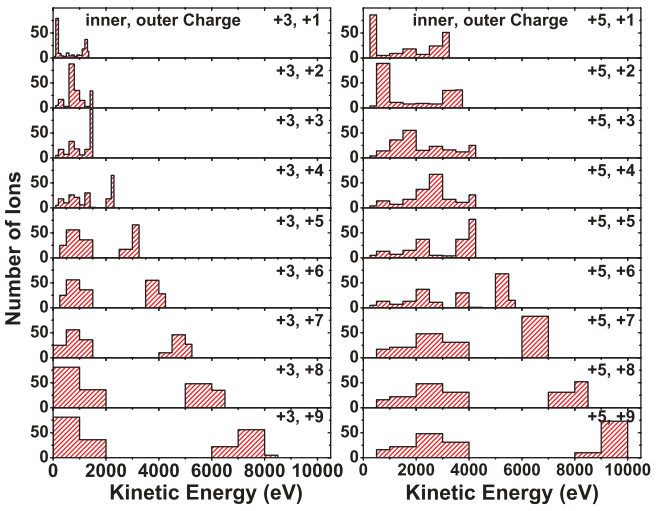

FIG. 4. (Color online) Simulation result of different charge-state combinations in a 200-atom argon cluster. The left side shows inner ions with a charge of 3+ while the charge of the outer ions is varied from 1+ to 9+; the right side shows the same outer charge variation with an inner-ion charge of 5+.

profile that originated from an inhomogeneous ion charge distribution inside the cluster after the laser interaction. The model assumed that all atoms in the cluster were ionized and started with a fixed charge that did not change with time. The initial positions of the ions were taken from the results of global optimizations for van der Waals clusters published by Wales *et al*. [15] and Xiang *et al*. [16,17]. To implement a simple radial charge distribution, all ions in the cluster were separated into two groups with a different degree of charge. One group represented ions that start from the inside of a sphere that has 80% of the cluster's initial radius and a second group included the rest of the ions that are in a shell outside this sphere. This corresponds to about 50% of the total number of ions in the cluster being in each region. The simulation then calculates the forces on every ion at each time step using a Runge-Kutta algorithm. The vertical ionization approximation was used, which assumes that, at the onset of the cluster expansion ($t = 0$), all ionized electrons are removed from the system and do not contribute to the expansion. Furthermore, it was assumed that all the remaining electrons are tightly bound to their atoms and thus do not contribute to the cluster expansion. Because of this ansatz, electrons were not explicitly treated in the model [18]. Since the energy of the particles was measured at large distances (at the detector position), the simulation was designed to calculate the motion and energy of individual particles until the interaction between the particles was small enough to have no significant effect on their energy.

With the assumption of this rough charge separation, the degree of charge for the inner and outer ions in the limits set by the observations in the TOF spectra of Fig. 2 was varied. The kinetic energy spectra produced by the simulation for a single cluster size resulted in a narrowly peaked energy profile where each peak corresponds to a shell of exploding ions because of the radially assigned charges within the cluster. An example of energy spectra from different charge combinations (inner versus outer) in a 200-atom argon cluster is shown in Fig. 4. The inner ions were assigned to a charge of 3+ (left) and 5+ (right), while the charge of the outer ions was varied from 1+ to 9+. Assuming a higher-charge state for the outermost ions led to more distinct energy profiles. An attempt to model two energy modes using a mixture of ion-charge states in the same radial shell was unsuccessful in that the two distinct modes could not be observed in the model.

In the measured spectrum for argon clusters with $\langle N \rangle = 200$, the high-energy peak around 5 keV and a peak for ions having energies <2 keV could be reconstructed best under the assumption that the inner half of the ions have a charge of 3+ while the outer-shell ions have a higher charge of 6+. To reproduce the measured energy spectrum, a rather broad log-normal distribution [11] around the mean cluster size of $\langle N \rangle = 200$ with full-width at half-maximum (FWHM) = $\langle N \rangle$ was included. The ions produced in all sizes of

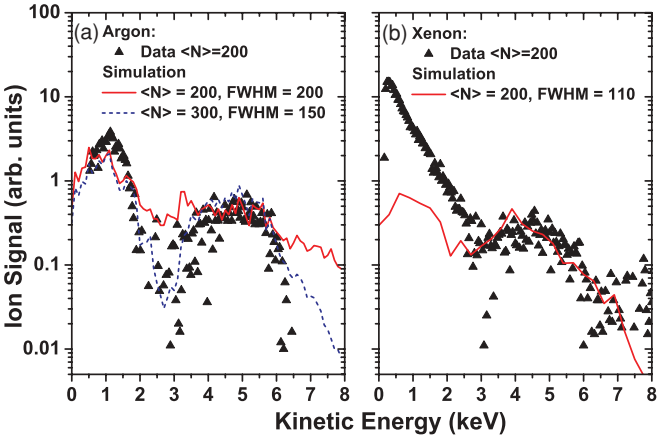

FIG. 5. (Color online) The bimodal peak structure in ion kinetic energy from exploding small clusters is reproduced by a simple classical particle simulation and fit to several log-normal size distributions. Ion energies are reproduced by a radial two-charge distribution, with charges of 3+ for the inner ions and 6+ for the outermost ions in (a) Ar clusters and 3+ for the inner ions and 7+ for the outermost ions in (b) Xe clusters.

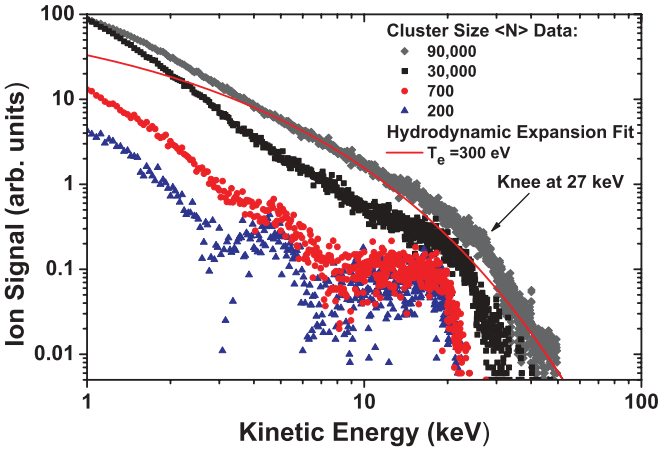

FIG. 6. (Color online) Ion kinetic energy spectra resulting from exploding xenon clusters. The largest cluster size is fitted to a quasineutral hydrodynamic expansion of a spherical cluster with an initial electron temperature of 300 eV.

simulated clusters consisting of 2 to 600 atoms were summed according to their abundance in the size distribution. This gave convoluted ion spectra that were capable of reproducing the measured data as shown in Fig. 5 (solid line). Applying a size distribution to other charge combinations did not reproduce the data. For example, the close, but less distinctive configuration of opposite charges, as shown in the +5, +2 combination of Fig. 4(b), resulted in an unstructured energy distribution. We also found that the simulated spectrum reproduced the experimental data better if we assumed a larger but narrower size distribution. For the $\langle N \rangle = 200$ atom cluster shown in Fig. 5(a) (dashed line), we assumed a log-normal size distribution with a mean cluster size of $\langle N \rangle = 300$ atoms and a FWHM of 150. This reproduced a more significant "dip" around 3 keV and matched the observed maximum kinetic energies of about 6 keV more accurately. The comparison between this simple model and the experiment is qualitative because the model ignores the presence of electrons during the cluster's expansion. A more complete model would be desirable, but is beyond the scope of this experiment. This charge distribution qualitatively supports a model by Jungreuthmayer *et al.* [19], which included all major microscopic and quantum effects in a three-dimensional particle in cell code for clusters of argon and xenon with several 10 000 atoms. This model predicted lower-charged ions in the inside due to screening by the space charge of free electrons, but higher-charge states on the outside shell of the cluster where the free electrons can leave the cluster more easily. These electron density variations locally increase the field strength and thus the ionization rate.

For xenon [Fig. 5(b)], the model was not able to reproduce the energy structure as well as in argon. The best fit shows a similar distribution with a 3+ inner charge and a 7+ outer charge. For the calculated cluster size of 200 atoms, energies of over 10 keV could not be reached under the assumption of reasonable charge states that are consistent with the measured TOF spectra. If we assumed that the mean cluster size was much bigger than 200, it would be possible to reproduce the spectrum (>1000 atoms per cluster, or significantly higher-charge states). Since the model was designed for smaller clusters, it was not capable of calculating a convolved energy spectrum corresponding to a mean cluster size of 1000 atoms or higher that would be needed to match the higher energy peak observed in the experiment. Also, at larger cluster sizes, our assumption of no trapped free electrons is no longer valid and the explosion dynamics changes. Instead, the higher energies observed in xenon clusters can be approximated using a hydrodynamic fluid model with one electron temperature by Schmalz [20] as shown for xenon with an electron temperature of 300 eV. However, this model does not produce the clearly pronounced "knee" observed at 27 keV in Fig. 6. Interestingly, according to Jungreuthmayer *et al.* [19] and Islam *et al.* [21], this knee results from the high-energy ions from a Coulomb explosion of a surface shell of ions in large clusters.

V. CONCLUSION

We presented detailed measurements on kinetic energy distributions of ions produced in rare-gas cluster explosions. Small clusters of argon and xenon (<700 atoms) showed a two-mode structure in the kinetic energy. A simple two-charge model reproduced the measured structure for $\langle N \rangle = 200$ clusters only when the charges reside in different radial shells, and if the higher-charge states lie at larger radius. This result is in agreement with more sophisticated models of laser-cluster interaction [19] that predicted lower-charged ions on the inside due to shielding space-charge effects, and higher-charge states on the outside of the cluster where the free electrons could leave it more easily. These electron density fluctuations locally increased the field strength and therefore the ionization.

[1] J. Purnell, E. M. Snyder, S. Wei, and A. W. Castleman Jr., Chem. Phys. Lett. **229**, 333 (1994).
[2] L. J. Frasinski, K. Codling, P. Hatherly, J. Barr, I. N. Ross, and W. T. Toner, Phys. Rev. Lett. **58**, 2424 (1987).
[3] A. N. Markevitch, D. A. Romanov, S. M. Smith, and R. J. Levis, Phys. Rev. Lett. **92**, 063001 (2004).
[4] T. Ditmire, T. Donnelly, A. M. Rubenchik, R. W. Falcone, and M. D. Perry, Phys. Rev. A **53**, 3379 (1996).
[5] T. Ditmire, J. W. G. Tisch, E. Springate, M. B. Mason, N. Hay, J. P. Marangos, and M. H. R. Hutchinson, Phys. Rev. Lett. **78**, 2732 (1997).
[6] H. M. Milchberg, S. J. McNaught, and E. Parra, Phys. Rev. E **64**, 056402 (2001).
[7] S. F. J. Larochelle, A. Talebpoury, and S. L. Chin, J. Phys. B: At. Mol. Phys. **31**, 1215 (1998).
[8] R. A. Smith, T. Ditmire, and J. W. G. Tisch, Rev. Sci. Instrum. **69**, 3798 (1998).
[9] F. Hagena and W. Obert, J. Chem. Phys. **56**, 1793 (1972).
[10] F. Dorchies, F. Blasco, T. Caillaud, J. Stevefelt, C. Stenz, A. S. Boldarev, and V. A. Gasilov, Phys. Rev. A **68**, 023201 (2003).

[11] M. Lewerenz, B. Schilling, and J. P. Toennies, Chem. Phys. Lett. **206**, 381 (1993).
[12] W. C. Wiley and I. H. McLaren, Rev. Sci. Instrum. **26**, 1150 (1955).
[13] K. Hoffmann, B. Murphy, B. Erk, A. Helal, N. Kandadai, J. Keto, and T. Ditmire, High Energy Density Phys. **6**, 185 (2010).
[14] T. Ditmire, Phys. Rev. A **57**, R4094 (1998).
[15] D. J. Wales and J. P. K. Doye, J. Phys. Chem. A **101**, 5111 (1997).
[16] Y. Xiang, H. Jiang, W. Cai, and X. Shao, J. Phys. Chem. A **108**(16), 3586 (2004).
[17] Y. Xiang, L. Cheng, W. Cai, and X. Shao, J. Phys. Chem. A **108**(44), 9516 (2004).
[18] I. Last and J. Jortner, J. Phys. Chem. A **106**(45), 10877 (2002).
[19] C. Jungreuthmayer, M. Geissler, J. Zanghellini, and T. Brabec, Phys. Rev. Lett. **92**, 133401 (2004).
[20] R. F. Schmalz, Phys. Fluids **28**, 2923 (1985).
[21] Md. Ranaul Islam, U. Saalmann, and J. M. Rost, Phys. Rev. A **73**, 041201(R) (2006).